

# Detection of subsurface defects of fused silica optics by confocal scattering microscopy

Bin Ma (马彬)<sup>1,2,3</sup>, Zhengxiang Shen (沈正祥)<sup>1,3</sup>, Pengfei He (贺鹏飞)<sup>2</sup>, Yiqin Ji (季一勤)<sup>3</sup>,  
Tian Sang (桑田)<sup>1,4</sup>, Huasong Liu (刘华松)<sup>1,3</sup>, Dandan Liu (刘丹丹)<sup>3</sup>,  
and Zhanshan Wang (王占山)<sup>1,3\*</sup>

<sup>1</sup>Institute of Precision Optical Engineering, Tongji University, Shanghai 200092, China

<sup>2</sup>School of Aerospace Engineering and Applied Mechanics, Tongji University, Shanghai 200092, China

<sup>3</sup>Tianjin Key Laboratory of Optical Thin Films, Tianjin Jinhang Institute of Technical Physics,  
Tianjin 300192, China

<sup>4</sup>Department of Physics, Qiannan Normal College for Nationalities, Duyun 558000, China

\*E-mail: wangzs@tongji.edu.cn

Received June 1, 2009

A non-destructive technique for subsurface measurements is proposed by combining light scattering method with laser confocal scanning tomography. The depth and distribution of subsurface defect layers are represented in term of scattered light intensity pattern, and three types of fused silica specimens are fabricated by different grinding and polishing processes to verify the validity and effectiveness. By using the direct measurement method with such technique, micron-scale cracks and scratches can be easily distinguished, and the instructional subsurface defect depths of 55, 15, and 4  $\mu\text{m}$  are given in real time allowing for an in-process observation and detection.

OCIS codes: 140.3330, 220.5450, 290.5825, 290.5850, 110.0180.

doi: 10.3788/COL20100803.0296.

During the initial figuring and shaping of optical components, optical processes of cutting and grinding are commonly required, and subsurface defects hiding beneath the top surface, such as cracks, scratches, and inclusions, are inevitable due to the brittle material removal mechanism. Even though in the polishing process, surface contamination particles and polishing powders may be imbedded in or near the surface, and the residual stress and strain may remain<sup>[1–3]</sup>. In application, the presence of subsurface defects may cause the highest-quality system failure, which will limit the performance of high power laser systems, so it must be eliminated from the surface. In order to achieve the ultimate removal, the accurate determination of distribution and depth of subsurface defect layer is needed. Numerous attempts have been made to develop efficient and reliable methods for detecting and assessing the character features below the surface<sup>[4–7]</sup>, including wet etching, total internal reflection microscopy, X-ray diffraction, quasi-Brewster angle technique, light scattering, and so on, which can be classified into destructive and non-destructive measurements. Moreover, many efforts have also been made to employ a series of post-processing steps to reduce or eliminate the subsurface defects.

In this letter, a light scattering method is improved to detect the intrinsic flaws of surface. It is shown that direct vertical information, including surface and subsurface signals, can be distinguished from each other using this method. As long as the unwanted light from above or below the focal plane is blocked<sup>[8,9]</sup>, scanning tomography of scattered light pattern caused by the defect structure in subsurface region can be obtained. After a series of images is recorded by varying the focal plane, vertical scene is recovered, and the  $x$ - $z$  or  $y$ - $z$  cross section at each

location could be constructed associated with the results of each image. This new technique, combining the light scattering method with laser confocal scanning tomography, is shown to be an effective and flexible method to detect the subsurface defect layer in term of intensity pattern, and micron-scale defects can be easily observed in a non-destructive and real-time way.

The effectiveness and feasibility of scattering measurements are based on the theory of light scattering by particles<sup>[10,11]</sup>. Light scattering of a particle will scatter in all different directions. Ignoring the multiple scattering, a polished substrate comprising numbers of randomly positioned defects in subsurface layer can be approximately dealt with and simply investigated in this way. However, in most cases the detector that measures scattered light is typically only sensitive to the light intensity which will disenable reappearing the original shapes of defects due to the lost phase. Therefore, the representation results by such method are usually in term of scattered light intensity pattern. Furthermore, the scattered light intensity generally has a direct dependence on defect size besides scattered angle. Thus, for subsurface defect detection, this dependence on size can be used to measure the scale of cracks and scratches hiding inside.

The validities of the confocal scattering technique to detect subsurface defect layer are discussed and verified in the following discussion. It is well known that the measured scattered light from a surface can be used to analyze the defect information, and a horizontal scanning is used to record the light intensity of the signal. However, no direct vertical measurement is made in this process, thus the information of surface and subsurface will be mixed with each other<sup>[12]</sup>.

An improved technique adapts the laser confocal scanning microscope system to achieve tomographic scanning by moving the focal plane focalized in the specimen. Both lateral and axial resolutions of confocal approach are approximate 1.44 times higher than that of conventional optical microscope, and the common expressions<sup>[13–15]</sup> of resolution based on Rayleigh criterion are

$$\Delta x_{\text{confocal}} = 0.4 \frac{\lambda}{\text{NA}}, \tag{1}$$

$$\Delta z_{\text{confocal}} = \frac{1.4\lambda n}{(\text{NA})^2}, \tag{2}$$

where  $\lambda$  is the light wavelength, NA is the numerical aperture of objective,  $n$  is the refractive index of the specimen.

The particular advantage of confocal microscope is the capability to obtain three-dimensional visualization because of the dramatic improvement in effective axial resolution over conventional techniques. In confocal configuration, a pinhole was placed in front of the detector, and only the focal plane can be detected, thus the picture was in black out of focus regions and did not contribute to the imaging. Then tomographic scanning was used to record a series of images by adjusting focal planes in  $z$  direction. Figure 1 shows a schematic illustration of such system.

Three kinds of fused silica specimens are fabricated using different grinding and polishing processes to verify the validity and accuracy of this non-destructive technique for assessing subsurface defects.

The specimen 1 is a ground surface grinded by brand W10 abrasive particles of SiC, with diameters in the range of 7–10  $\mu\text{m}$ . In order to eliminate the defect layer introduced by previous operations, the total removal depth needs to reach hundreds of microns by W10 abrasive particles. But the knife-edged shape and stiff texture of SiC grains used in current grinding approach will also leave a new surface ductile layer with dislocation structures simultaneously.

Figure 2(a) presents the measured results by the non-destructive technique using the intensity of scattered light to assess the subsurface defect distribution of

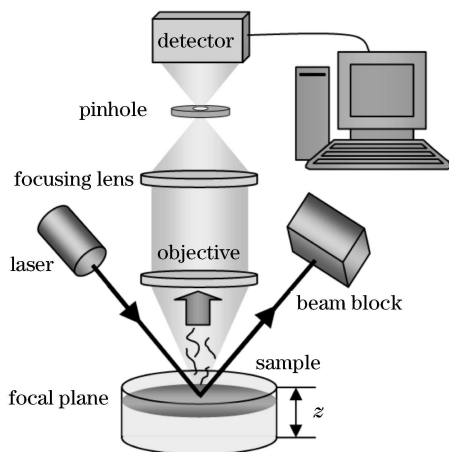


Fig. 1. Schematic of a non-destructive subsurface measurement system.

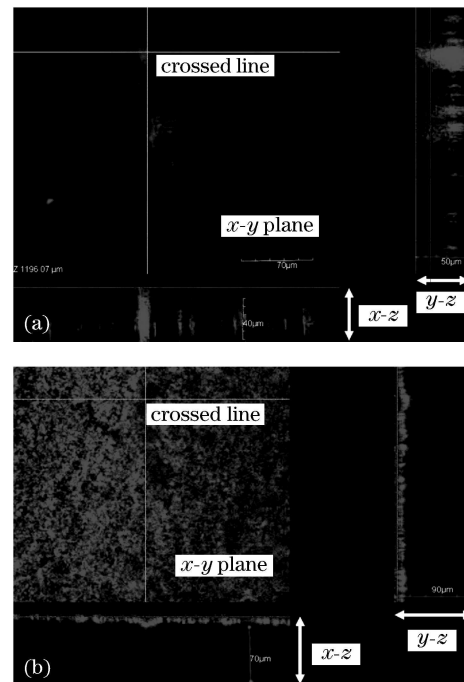


Fig. 2. Subsurface defect distributions. (a) Specimen 1 and (b) specimen 2.

specimen 1. The crossed line is the location of  $x$  and  $y$  images, the bottom and right parts display the measured graphs of  $x$ - $z$  and  $y$ - $z$  planes along the crossing position, respectively. By detecting the scattered light induced by defect structure, the subsurface defect layer can be described in intensity distribution. The focal plane is adjusted vertically in the distance of  $\sim 1200 \mu\text{m}$ . Consequently, a scattered layer with a thickness of  $55 \mu\text{m}$  near the top surface can be observed. The cross sections,  $x$ - $z$  and  $y$ - $z$  planes exhibit similar scattered patterns according to the position in  $x$ - $y$  plane, and the enhanced or increased intensity signals indicate light scattered from a defect or damage at each observation point within the measured area. Moreover, the light intensity corresponds to the severity of defects, and an extremely severe defect structure may make the charge-coupled device (CCD) overloaded, resulting in darker display in the other regions.

The specimen 2 is also a ground surface but grinded by W5 of SiC, and the diameters of particles are mainly in the range of 3.5–5  $\mu\text{m}$ . The defect layer produced in W10 grinding process has been wiped off by enough removal depth. Similarly, the new defect layer caused by the W5 grinding process is also measured, as shown in Fig. 2(b).

Owing to the smaller abrasives, the characteristic of new defect layer is a little different from that of the defect layer caused by W10 abrasives. The structure becomes more exiguous but more compact which is also can be shown by the scattered light intensity. A sufficient scanning distance in vertical cross section has been executed, and a defect layer with thickness of approximate  $15 \mu\text{m}$  can be observed.

Generally, grinding is widely used in shaping optical components because of its high removal rate. Unfortunately, due to the brittle material removal mechanism

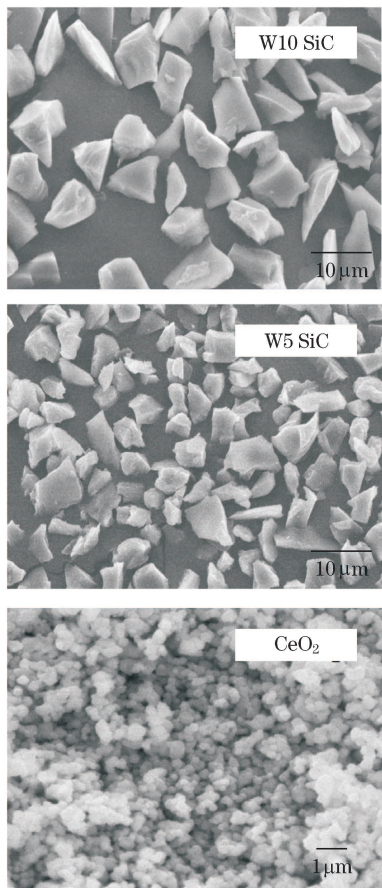


Fig. 3. SEM images of SiC abrasive particles and CeO<sub>2</sub> polishing powders.

in grinding operation, fragile specimen, and sharp abrasives, the subsurface defects are always inevitably introduced. However, the subsurface defects can be minimized throughout the grinding process by a series of grinding steps with successively smaller abrasives. In application, the decrease of abrasives size will lead to the better surface quality, and a more slight subsurface defect structure can be obtained. To successfully eliminate the subsurface defect layer, the removal depth should be higher than that of the residual defects, and the defect properties in the grinding process are very important. From the measurement results given above, W10 SiC abrasives may result in a defect layer with thickness higher than 55 μm while W5 abrasives may induce a nearly 15-μm-thick layer. The introduced depth of the defect layer is related to the abrasives size with 4–6 times of the basic diameter commonly according to the results mentioned above.

Whereafter, polishing process is implemented to remove previous subsurface defects without introducing additional severe defects. We note that the appearance of polishing powders are distinctly different from the grinding abrasives, as shown in Fig. 3.

In Fig. 3, the size of individual CeO<sub>2</sub> powder is only about several hundreds of nanometers with regular shape, soft edge, and flexible texture by ignoring the clustered states, and may be broken up potentially during polishing process.

The specimen 3 was fabricated as a polished surface

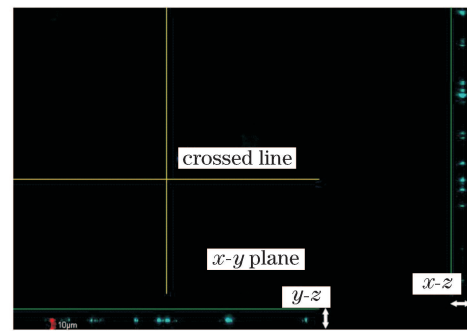


Fig. 4. Subsurface defect distribution of specimen 3.

with 0.5-nm root-mean-square (RMS) roughness without sufficient removal depth. Considering that the slight defect structure leading to a tiny signals of the scattered light, the illuminated light source, 10-mW He-Ne laser, was replaced by 30-mW Ar laser. Figure 4 exhibits the intensity pattern.

In Fig. 4, the new technique enables to capture obscure cracks and scratches hiding in the subsurface after polishing operation. The image indicates the location of the defects in vertical cross section down through *x-z* or *y-z* plane. Obviously, a change in the defect density indicates a change in the size of the flaws or fractures in each grinding process. Unfortunately, each of the isolated flaws or scratches near surface region cannot be characterized in terms of the length that it extends inside. The isolated intensity signals only represent the location and approximate sizes of cracks and scratches, which is invalid for their micro-shape and real appearance. But the directive results have proved that defects around 4 μm deep and several microns wide can be easily distinguished for the specimen 3.

Furthermore, if the specimen 3 is polished again with the survived defect layer being wiped off, in this case, the scattered intensity signal will be too weak to record, and the total dark field will appear.

In conclusion, a non-destructive and real-time subsurface measurement system has been set up based on light scattering method and laser confocal scanning microscopy. Scattered light from defect structure is collected to character the subsurface quality. By adjusting the focal plane in vertical distance within the specimens, the laser confocal scanning tomography can be used to exhibit the cross section of *x-z* or *y-z* plane of each location. Three kinds of specimens fabricated by grinding and polishing process are investigated, and the validity and effectiveness of this non-destructive and real-time subsurface measurement method are verified. Instructional depths of 55, 15, and 4 μm are given for these three types of specimens. The measurement system based on light scattering method can provide the rough distribution of cracks and scratches, although it is incapable of converting the observed patterns to the actual profiles. In study of detailed shape and property of all types defect layer, the phase information of scattered light must be considered.

Technical support from Olympus is gratefully acknowledged. This work was supported by the National Natural Science Foundation of China (No. 10825521), the Na-

tional "863" Program of China (No. 2006AA12Z139), and the Shanghai Committee of Science and Technology (No. 07DZ22302).

## References

1. P. E. Miller, T. I. Suratwala, L. L. Wong, M. D. Feit, J. A. Menapace, P. J. Davis, and R. A. Steele, Proc. SPIE **5991**, 599101 (2005).
2. T. Suratwala, L. Wong, P. Miller, M. D. Feit, J. Menapace, R. Steele, P. Davis, and D. Walmer, J. Non-Cryst. Solids **352**, 5601 (2006).
3. D. Golini and S. D. Jacobs, Proc. SPIE **1333**, 80 (1990).
4. C. L. Battersby, L. M. Sheehan, and M. R. Kozlowski, Proc. SPIE **3578**, 446 (1998).
5. Z. M. Liao, S. J. Cohen, and J. R. Taylor, Proc. SPIE **2428**, 43 (1995).
6. D. Black, R. Polvani, L. Braun, B. Hockey, and G. White, Proc. SPIE **3060**, 102 (1997).
7. J. Wang, R. L. Maier, and J. H. Burning, Proc. SPIE **5188**, 106 (2003).
8. G. Dussler, B. Brocher, and T. Pfeifer, Proc. SPIE **3825**, 144 (1999).
9. T. Zamofing and H. Hügli, Proc. SPIE **5265**, 134 (2004).
10. M. I. Mishchenko, L. D. Travis, and A. A. Lacis, *Scattering, Absorption, and Emission of Light by Small Particles* (Cambridge University Press, Cambridge, 2004).
11. K.-N. Liou, Appl. Math. Comput. **3**, 331 (1977).
12. K. R. Fine, R. Garbe, T. Gip, and Q. Nguyen, Proc. SPIE **5799**, 105 (2005).
13. J. Neauport, P. Cormont, P. Legros, C. Ambard, and J. Destribats, Opt. Express **17**, 3543 (2009).
14. K. R. Spring, T. J. Fellers, and M. W. Davidson, "Resolution and contrast in confocal microscopy" <http://www.olympusconfocal.com/throry/resolutionintro.html> (Jan. 8, 2009).
15. P. Török and T. Wilson, Opt. Commun. **137**, 127 (1997).